

Published in final edited form as:

J Immunol. 2021 April 01; 206(7): 1549–1560. doi:10.4049/jimmunol.2001066.

Niche mediated integrin signaling supports steady state hematopoiesis in spleen

Shubham Haribhau Mehatre¹, Irene Mariam Roy^{#1}, Atreyi Biswas^{#1}, Devila Prit¹, Sarah Schoutedden², Joerg Huelsken³, Catherine M. Verfaillie², Satish Khurana^{1,*}

¹School of Biology, Indian Institute of Science Education and Research Thiruvananthapuram, Kerala, India 695551

²Inter-departmental Stem Cell Institute, KU Leuven, 3000 Leuven, Belgium

³École Polytechnique Fédérale de Lausanne (EPFL), 1015 Lausanne, Switzerland

These authors contributed equally to this work.

Abstract

Outside-in integrin signaling regulates cell fate decisions in a variety of cell types, including hematopoietic stem cells (HSCs). Our earlier published studies showed that interruption of Periostin (POSTN) and Integrin- α v (ITGAV) interaction induces faster proliferation in HSCs with developmental stage dependent functional effects. Here, we examined the role of POSTN-ITGAV axis in lympho-hematopoietic activity in spleen that hosts rare population of HSCs, the functional regulation of which is not clearly known. *Vav-iCre* mediated deletion of *Itgav* in hematopoietic system led to higher proliferation rates, resulting in increased frequency of primitive HSCs in adult spleen. However, *in vitro* CFU-C assays demonstrated a poorer differentiation potential following *Itgav* deletion. This also led to a decrease in the white pulp area with a significant decline in the B-cell numbers. Systemic deletion of its ligand, POSTN, phenocopied the effects noted in *Vav-Itgav*^{-/-} mice. Histological examination of *Postn* deficient spleen also showed increase in the spleen trabecular areas. Importantly, these are the myofibroblasts of the trabecular and capsular areas that expressed high levels of POSTN within the spleen tissue. In addition, vascular smooth muscle cells also expressed POSTN. Through CFU-S₁₂ assays, we showed that hematopoietic support potential of stroma in *Postn* deficient splenic hematopoietic niche was defective. Overall, we demonstrate that POSTN-ITGAV interaction plays important role in spleen lympho-hematopoiesis.

*Correspondence: Satish Khurana, PhD, Wellcome trust-DBT India Alliance Fellow and Assistant Professor, School of Biology, Indian Institute of Science Education and Research Thiruvananthapuram, Kerala, India 695551, Tel: +91-471-2778046, satishkhurana@iisertvm.ac.in.

Author Contribution

SK designed and supervised the study, wrote the manuscript. CMV provided material and reviewed the manuscript. SHM and DP performed the experiments and analyzed the results. IMR and SS provided assistance with flow cytometry experiments. AB provided assistance with IHC experiments. JH provided material.

Declaration of Interests

The authors declare no competing interests.

Introduction

In adult mammals, blood cell production takes place in the bone marrow (BM), wherein the hematopoietic stem cells (HSCs) reside and function, taking cues from extrinsic factors (1). During the onset of postnatal hematopoiesis, thymus takes up specialized function of lymphopoiesis, while spleen shows compartmentalization into lymphopoietic and non-lymphopoietic zones (2). Both of these zones show developmental as well as structural distinctions and support remarkable differences in function. Although spleen acts as a secondary lymphoid organ that plays a crucial role in both innate and adaptive immune system functions, neonatal splenectomy did not alter essential hematopoietic processes (3). Apart from the active hematopoietic events during embryonic development or immune-activation, spleen undertakes extramedullary hematopoiesis (EMH) during BM failure in several pathological conditions, pregnancy and blood loss (4).

It is believed that EMH involves migration of HSCs from their normal niches; and homing, proliferation and differentiation supported by the extramedullary sites (5). In this process, a role of activated macrophages in modulating the capacity of spleen niche to support incoming HSCs was demonstrated. Silencing of the receptor for macrophage-colony stimulating factor (M-CSF) through nanoparticle encapsulated siRNA that caused decrease in the macrophage numbers, led to a reduction in spleen resident HSCs (6). This study further showed that M-CSF silencing selectively decreased the expression of vascular cell adhesion molecule 1 (VCAM-1), primarily expressed by macrophages in spleen. VCAM-1 is a ligand for integrin heterodimer VLA-4 (Very Late Antigen-4, integrin- $\alpha 4\beta 1$) (7), well known for its role in homing, maintenance and functioning of HSCs in the BM (8). Inhibition of VLA-4 using small molecule inhibitors (9) or specific antibodies (10) induced mobilization of HSCs. Integrins are one of the most important classes of cell surface receptors that mediate HSC interaction with their niche through outside-in and inside-out signaling mechanisms (11, 12).

Although it was reported that HSCs might follow distinct mechanisms for homing and functioning in the BM and spleen niche (13), evidence suggested that integrin signaling was important for the establishment of hematopoietic activity in embryonic spleen (14). Even homing of transplanted HSCs into spleen, similar to the BM, was shown to be mediated via interaction of HSCs with their niche through integrins (8). Therefore, the importance of cell adhesion, mediated by inside-out integrin signaling, in hematopoietic processes in BM and spleen has been known. In contrast, the evidence of involvement of ligand mediated outside-in integrin signaling is not clearly elucidated. The importance of Osteopontin (OPN), a known factor that elicits outside-in integrin signaling as a negative regulator of HSC function, has been well established (15, 16). OPN binds to a variety of integrin heterodimers, most important being the ones with integrin- αv (ITGAV) as one of the monomers (17). In our recent findings, Periostin (POSTN) that shows binding specificity to ITGAV-containing integrin heterodimers (18), is demonstrated as a negative regulator of HSC proliferation (12). However, another study reported the involvement of integrin- $\alpha v\beta 3$, synergizing the effect of interferon- γ (IFN- γ) on HSC proliferation, resulting in the loss of hematopoietic function (19). In fact, a clear role of ITGAV in TGF- β mediated T-cell stimulation to mount Th17 response has been elucidated (20). Lack of *Itgav* expression

inhibited auto-immune response in experimental autoimmune encephalomyelitis (EAE) model. Interestingly, POSTN has also been shown to mediate allergen induced inflammatory response in skin (21). Inhibition of POSTN or ITGAV resulted in complete abrogation of allergen-induced skin inflammation. However, the involvement of POSTN-ITGAV mediated outside-in integrin signaling in splenic HSC function has not been established yet.

Spleen is a major site for extra-medullary hematopoiesis (EMH), where HSCs mobilized from the BM play an important role. In this context, the role of spleen resident HSCs, a rather rare population, is not well documented. It is important to note that at the cellular level, spleen resident HSCs have been reported to possess function, equivalent to the BM HSCs (22). However, their function in maintaining the supply of mature blood cells is not clearly known and regulatory pathways remain elusive. Here we show that POSTN, expressed majorly in the myofibroblasts of the splenic capsule and trabeculae, is involved in spleen lympho-hematopoietic activity. Lack of its receptor, ITGAV, led to increased proliferation rate in HSCs and decrease in the B-cell population with concomitant increase in the megakaryocyte numbers. POSTN deficiency largely mimicked the phenotype with additional defects in the spleen hematopoietic niche that led to poorer support for the incoming hematopoietic progenitors. Overall, we show that ITGAV-mediated outside-in integrin signaling plays an important role in the steady state hematopoietic activity in spleen.

Materials and methods

Mice

Twelve to sixteen week-old FVB/NJ, C57BL/6J-CD45.2 (*Centre d'Élevage R. Janvier, Le Genest-St Isle, France*), and *Postn*^{-/-} mice (23) were maintained in the animal facilities at IISER TVM and KU Leuven. *Itgav*^{flox/flox} mice (24) were crossed to *Vav-iCre* mice (25) from Thomas Graf, Centre for Genomic Regulation, Barcelona) to obtain *Vav-iCre;Itgav*^{fl/fl} mice. Genotyping was performed on genomic DNA from tail tips, as described before (12). The complete list of primers used for genotyping is provided in Supplementary table 1. *Vav-iCre*⁻;*Itgav*^{fl/fl} and *Vav-iCre*⁺;*Itgav*^{+/+} littermates were used as controls. During the experiments, mice were maintained in isolator cages, fed with autoclaved acidified water and irradiated food ad libitum. All procedures involving the use of animals were approved by the Institutional Animal Ethics Committees (IAEC) of IISER TVM and KU Leuven. At IISER TVM, experiments were conducted following the guidelines of the Committee for the Purpose of Control And Supervision of Experiments on Animals (CPCSEA), Government of India.

Flow cytometry

Hematopoietic lineage analysis of spleen cells was performed by flow cytometry, using specific antibodies. Cell cycle analysis was performed by Hoechst 33342 (Ho; 10µg/ml) and Pyronin Y (PY; 1µg/ml) staining (26), in addition to labelling with Hematopoietic stem and progenitor cell (HSPC) (LSKs; Lin⁻Sca-1⁺c-kit⁺ cells) or HSC Hematopoietic stem cell (SLAM LSKs; CD150⁺CD48⁻Lin⁻Sca-1⁺c-kit⁺) markers. Lineage specific antibodies used were FITC conjugated Mac-1 and Gr-1 for myeloid cells, PEcy7 conjugated B220 for B-cells, PE conjugated anti-CD4 and anti-CD8 for T-cells were used. All antibodies were

procured from BD Pharmingen at were used at 0.25µg/ml concentration. Flow cytometric analysis for HSPC populations was performed using APC conjugated lineage antibody cocktail, PE conjugated anti mouse c-kit, PerCPCy5.5 conjugated anti-mouse Sca-1, FITC conjugated anti-mouse CD48 and PECy7 conjugated CD150 (0.25µg/ml; ebiosciences) antibodies. ITGAV and ITGB3 expression in the spleen derived HSCs were analyzed by using α-mITGAV and α-mITGB3 antibodies along with primitive HSC markers. Suitable isotype controls for each antibody were used in all experiments. Complete list of antibodies used for these experiments is provided in Supplementary table 1. The cells were analyzed by flow cytometry using FACS Aria III (BD Biosciences, San Jose, CA) and FlowJo software (TreeStar, Ashland, OR). For all analyses, debris and platelets were excluded by setting up suitable threshold while acquiring the samples. In addition, low FSC-A cells were gated out to further analyze the splenocytes for various marker expressions.

Quantitative RT-PCR

Total RNA was prepared using the RNA Isolation Kit (Qiagen, Hilden, Germany), according to the manufacturer's protocol. 100ng-1µg of RNA from each sample was used to synthesize cDNA using PrimeScript™ RT Reagent kit (Takara Bio Inc., Japan). Quantitative RT-PCR was carried out using TB Green™ Premix EX Taq™ II (Takara Bio Inc., Japan). The PCR reactions were carried out in a CFX96 detection system (Thermal-Cycler C1000, Bio-Rad, Hercules, CA, USA). List of primers used is provided in Supplementary table 1.

Radiation injury and colony-forming unit-spleen (CFU-S) assay

A single dose of 4.5 Gy (sub-lethal dose) radiation on a Rad Source RS-2000 Biological Irradiator (Rad Source Technologies, Alpharetta, GA) was given to the animals to induce hematopoietic injury. Splenic HSPC population in *Postn*^{+/+} and *Postn*^{-/-} mice was examined using methylcellulose-based colony assay a week after irradiation dose was given.

For CFU-S₁₂ assays, recipient *Postn*^{+/+} and *Postn*^{-/-} mice were lethally (10Gy) irradiated and injected with 1x10⁵ control FVB/NJ mouse BM derived cells. Three recipient animals were used for each donor mouse and the experiment was repeated thrice. Recipients were sacrificed 12 days after injection. Spleen colonies (CFU-S₁₂) were visualized and counted as described before (27).

Histological and immunofluorescence studies

The spleen tissues were harvested, washed in PBS and fixed with 4% paraformaldehyde (PFA) overnight at 4°C and washed with phosphate buffered saline (PBS) and stored. The fixed tissues were dehydrated through gradient of ethanol and were cleared using xylene followed by paraffin infiltration. Paraffin blocks were made by embedding tissue in molten Paraplast X-Tra® using a Leica EG1150 Modular Tissue Embedding Centre. For histological analysis, 10µm thick tissue sections were cut using a microtome (Leica RM2265). FFPE sections on glass slides were stained with Harris' hematoxylin (HHS16; Sigma Aldrich) and eosin solution (HT110116; Sigma Aldrich). The sections were mounted using DPX mounting medium (DB6DF66104; MERCK) for microscopy. Brightfield images were captured on an Olympus IX83 inverted microscope, using 40X objective (UPlan FL

N_{40x/0.75_∞/0.17/FN26.5}). CellSens Dimension 2.3 (Build 18987) software was used to capture and analyses of images.

Immunohistochemistry and imaging: Spleen tissues were harvested and washed in PBS and fixed with 4% paraformaldehyde (PFA) for 2 hours on shaker at ice-cold temperature and washed with PBS three times at 10 minutes interval and stored in 0.1% Sodium azide (Sigma_71289-50G) solution in PBS at 4°C. Fixed tissues were subjected to 48 hours 30% sucrose gradient for cryo-protection prior to cryo-block preparation using Polyfreeze (Sigma_P0091). Cryotome (Thermo Scientific HM525 NX) was used to obtain 10µm thick sections on frosted slides (VWR_631-0108). Immuno-labelling was performed using antigen specific primary antibodies; anti-periostin antibody (R&D systems, Minneapolis, MN), anti-α-smooth muscle actin antibody (abcam), anti-CD31 antibody (R&D systems, Minneapolis, MN), anti-collagen IV antibody (abcam), anti-laminin antibody (abcam) and fluorophore-conjugated secondary antibodies (Jackson ImmunoResearch Laboratories Inc.) For each experiment, appropriate matched-isotype antibody controls were used (Suppl. Fig. 1A-C). Hoechst 33342 (Sigma) was used to counterstain the nuclei. Sections were mounted using ProLong™ Gold antifade mounting medium (Invitrogen_P36934). Fluorescence imaging was performed using Leica TCS SP5 II upright confocal microscope. Images were captured using 63X oil immersion objective (HCX PL APO CS 63.0x1.40 Oil) by software LAS AF. Leica Application Suit X (Version: 3.3.016799) software was used for analyzing the obtained images.

Statistical analysis

Normal distribution of data was tested using the Shapiro-Wilk test. The data with normal distribution is represented as mean ± s.e.m. Data with non-normal distribution was represented in box-and-whisker plots, indicating median in the box with 25th and 75th percentile (in box) and minimum and maximum values (top and bottom whiskers respectively). The equality of group variance was tested using Brown-Forsythe test. Comparisons between samples from two groups with normally distributed data with equal variance were made using the unpaired two-tailed Student's *t-test*. Mann Whitney test was used for comparing two groups where data were non-normally distributed. For multiple comparisons of the normally distributed data with equal variance, one-way ANOVA was performed followed by Tukey Kramer post hoc test. Non-normally distributed data was analyzed by Friedman test. Statistical analyses were performed with Microsoft Excel or GraphPad Prism 6. For all analyses, p-value 0.05 was accepted as statistically significant.

Results

POSTN is expressed by capsular and trabecular myofibroblasts

We first examined the spatial localization of POSTN in the spleen tissue by performing immunohistochemistry using anti-POSTN antibodies. As spleen is functionally divided into two major regions, white pulp (WP; for lymphopoiesis) and red pulp (RP; for blood filtration), we tested if the expression of POSTN was restricted to one of these regions. We used anti-CD169 antibodies to detect macrophages of the marginal zone that clearly demarcate WP from RP (28, 29). We performed tile scans of the transverse sections of

spleen and observed that the expression of POSTN (isotype antibody controls for each antibody are shown in Suppl. Fig. 1A-C) was mostly limited to the RP (Suppl. Fig. 1D). However, modest level of POSTN expression was observed in the vascular region of WP as well. Preliminary observations indicated that POSTN expression might be associated with the capsular, trabecular and vascular regions of the spleen tissues. To confirm this, we used anti- α -smooth muscle actin (α -SMA) antibodies to identify specific cells and splenic regions with POSTN expression (Fig. 1A). We confirmed that POSTN expression was mostly but not completely confined to the RP area. We also observed that the myofibroblasts of the capsular (Fig. 1B) and trabecular regions (Fig. 1C), as well as the smooth muscle cells of the vasculature (Fig. 1D) showed significant levels of POSTN expression. Although capsular myofibroblasts expressed lower levels of POSTN, all α -SMA⁺ cells in the spleen tissue were seen to express POSTN. Our recent findings showed that vascular endothelium was the key source of POSTN in the fetal liver (FL) HSC niche, with no significant expression seen in the vascular smooth muscle cells (30). Therefore, we tested if the vascular endothelium, in addition to the smooth muscle cells associated with vasculature expressed POSTN. We noted that the endothelial lining (CD31⁺) of the blood vessels did not express POSTN while the surrounding α -SMA⁺ cells showed high level of POSTN expression (Fig. 1E). These results show that cellular source of POSTN may vary between different tissues or developmental stages.

As POSTN is an extracellular matrix (ECM) binding protein, we examined its association with two of the most common ECM proteins in spleen tissue, Laminin and Collagen IV, in different anatomical locations within the tissue (Fig. 2). Distribution pattern of the two proteins in vascular region was similar, except for the vascular basal lamina that was composed mainly of laminin. Importantly, there was no clear preferential co-localization of POSTN with either laminin (Fig. 2A, upper panel) or COL IV (Fig. 2A, lower panel). Rather, it appeared to be determined by the closeness to the POSTN expressing cells. Therefore, ECM associated POSTN was more closer to the smooth muscle cells underneath the endothelial layer (white arrows) of the vessel. In the case of trabecular (Fig. 2B, upper and lower panel) as well as lymphopoietic WP area (Fig. 2C, upper and lower panel), POSTN localization was not determined by the ECM proteins rather by the presence of smooth muscle cells/myofibroblasts in the region.

ITGAV and ITGB3 are expressed in the spleen hematopoietic stem cells

We next performed flow cytometry analysis to examine the expression of ITGAV and ITGB3 in different sub-populations of spleen resident hematopoietic stem and progenitor cells (HSPCs; Figure 3). On the basis of expression of SLAM markers, CD150 and CD48, lin⁻c-kit⁺Sca-1⁺ (LSK) population was subdivided into four sub-populations; CD150⁺CD48⁻ (P1), CD150⁺CD48⁺ (P2), CD150⁻CD48⁺ (P3) and CD150⁻CD48⁻ (P4) (Fig. 3A). Subsequently, the expression of ITGAV (Fig. 3B, upper panel) and ITGB3 (Fig. 3B, lower panel), in each of these populations was examined (isotype controls for each antibody are shown in Suppl. Fig. 1E,F). Results showed that among all the sub-populations, primitive HSCs (P1) expressed the highest level of ITGAV expression (57.46±3.55%). However, the short-term (ST-) HSCs (P4; 36.06±3.21%) as well as other multipotent progenitors (P2; 38.58±4.44% and P3; 26.42±2.83%, and) also expressed significant levels of the protein

(Fig. 3C). As ITGAV has been shown to partner with ITGB3 to form a heterodimeric integrin receptor in a variety of cell types (31), including a number of cancers (32), we investigated the expression of ITGB3 in the stem cell sub-populations. We observed that the proportion of most primitive HSCs (P1) that expressed ITGB3 ($68.88 \pm 3.97\%$) was higher than both $CD150^+CD48^+$ ($50.96 \pm 3.7\%$) and $CD150^-CD48^+$ ($37.82 \pm 4.3\%$) LSK sub-populations (Fig. 3C). Thus, a significant proportion of all sub-populations, most importantly the primitive HSCs, expressed ITGAV and ITGB3. To confirm the co-expression of ITGAV and ITGB3 on primitive HSCs, we repeated flow cytometry experiments. The primitive HSCs (P1) was analyzed for the expression of both of the integrin chains (Fig. 3D,E). We observed that $31.70 \pm 2.81\%$ of the most primitive spleen resident HSCs co-expressed ITGAV and ITGB3. Of note, $49.41 \pm 3.09\%$ of the HSCs that expressed ITGAV also expressed ITGB3 (Fig. 3E).

In order to understand if POSTN-ITGAV interaction played any role in spleen lymphohematopoietic activity, we conditionally deleted *Itgav* in hematopoietic cells by crossing *Itgav^{fl/fl}* (24) with *Vav-iCre* mice (25). Genotyping was performed on the DNA isolated from tail tip tissues of adult animals and *Vav-Itgav^{+/+}* and *Vav-Itgav^{-/-}* mice were identified and used for further analysis (Suppl. Fig. 2A-C). We confirmed the loss of ITGAV expression in the splenic HSPC population by flow cytometry (Suppl. Fig. 2D). Spleen derived LSK cells were examined for cell surface expression of ITGAV and comparison was made between *Vav-Itgav^{+/+}* and *Vav-Itgav^{-/-}* mice. Results showed significantly reduced expression of ITGAV on HSPCs from *Vav-Itgav^{-/-}* mice (Suppl. Fig. 2D). Initial observations suggested little change in the gross morphology of spleen, upon *Itgav* deletion (Fig. 3F). However, we observed a modest increase in spleen weight (Fig. 3G) and total cellularity (Fig. 3H). Analysis of the transverse sections through the tissue showed an increase in the cross-sectional area (Fig. 3I).

***Itgav* deletion leads to increased HSC proliferation and poorer lymphopoietic function**

To examine the effect of loss of ITGAV in spleen hematopoietic system, we compared *Vav-Itgav^{+/+}* and *Vav-Itgav^{-/-}* mice for the frequency of HSPCs (lin^-c-kit^+ cells; Suppl. Fig. 2E), LSK cells and primitive HSCs in spleen tissues (Fig. 4A-C). Although we did not observe any significant change in the frequency of lin^-c-kit^+ cells (Suppl. Fig. 2E), we did observe a significant increase in the frequency of LSK cells (Fig. 4B) as well as primitive HSCs (Fig. 4C) following *Itgav* deletion. We then examined if this increase in the frequencies of HSPC populations was accompanied by an altered proliferation status. Cell cycle analysis of the control spleen derived mononuclear cells (MNCs), using Hoechst and Pyronin Y staining (Fig. 4D,E), showed $64.23 \pm 1.44\%$ of the spleen resident primitive HSCs to be quiescent (in G0 stage). Upon *Itgav* deletion, we observed a significant decrease in the proportion ($49.44 \pm 1.48\%$) of quiescent HSCs (Fig. 4E). No significant difference upon *Itgav* deletion was observed in the proportion of spleen HSCs in G1 phase of cell cycle ($20.74 \pm 1.44\%$ in WT and $26.64 \pm 1.96\%$ in *Vav-Itgav^{-/-}*). However, we observed an increase in the proportion of cells in S phase, from $9.44 \pm 1.33\%$ to $13.45 \pm 0.67\%$ and in G2/M phase, from $5.59 \pm 0.042\%$ to $10.48 \pm 1.58\%$ upon *Itgav* deletion in hematopoietic system (Fig. 4E). These results indicate that the loss of ITGAV in the hematopoietic system leads to increased proliferation rates. We next examined a possible impact of increased proliferation rates on

the function of stem cell population by performing methylcellulose-based colony assays (Fig. 4F,G). Results showed no difference in total colonies formed (Fig. 4F) but the number of CFU-GEMMs per spleen (Fig. 4G) was significantly decreased, showing a functional decline in more primitive progenitors in the spleen, following *Itgav* deletion.

Our earlier published results showed significant loss of long-term engraftment potential in the *Vav-Itgav*^{-/-} HSCs from BM, with concomitant loss of lymphocytes in peripheral blood (12). Here, we performed experiments to understand if *Itgav* deletion led to any loss of lympho-hematopoietic activity in spleen. We first performed H&E staining based histological analysis on 10µm thick spleen sections (Fig. 4H) and observed a significant decrease in the WP area (Suppl. Fig. 2F) and a corresponding increase in the RP area (Suppl. Fig. 2G) upon *Vav-iCre* induced *Itgav*-deletion. This resulted in an overall increase in the RP/WP ratio in the spleen tissues from *Vav-Itgav*^{-/-} mice (Fig. 4I). Splenic WP area is associated with lymphopoietic activity. To confirm any change in T- or B- lymphopoietic activity, we performed flow cytometry analyses of the MNCs from spleen tissue (Fig. 4J-M). We observed increase in the myeloid population (CD11b/Gr-1⁺) in *Vav-Itgav*^{-/-} spleen (Fig. 4K). While no difference was observed in T-cell population (CD4/CD8⁺; Fig. 4L), *Itgav*-deletion led to a significant decrease in the B-cell population (B220⁺; Fig. 4M). Careful observations on the spleen tissue sections from *Vav-Itgav*^{-/-} mice showed an increase in the megakaryocyte frequency compared to the control (Suppl. Fig. 2H,I).

Postn deletion partially mimics the effects observed in *Vav-Itgav*^{-/-} mice

To confirm that the effects of *Itgav* deletion reflected the importance of POSTN-ITGAV interaction specifically, we analyzed spleen hematopoietic system following *Postn* deletion. Lack of *Postn* expression in the spleen tissue was confirmed by performing quantitative RT-PCR on magnetically isolated lin⁻CD45⁻ fraction of splenocytes (Suppl. Fig. 3A). We did not detect POSTN expression in the *Postn*^{-/-} samples. Surprisingly, unlike in the case of *Vav-Itgav*^{-/-} mice, *Postn*^{-/-} mice showed significantly smaller spleens (Fig. 5A), as can be seen through a significant decrease in spleen weight (Fig. 5B), total cellularity (Fig. 5C) as well as average cross-sectional area (Fig. 5D). Next, we performed flow cytometry experiments (Fig. 5E) to examine the frequency of HSPCs (lin⁻c-kit⁺ cells; Suppl. Fig. 3B), LSKs (lin⁻c-kit⁺Sca-1⁺ cells; Fig. 5F) and primitive HSCs (CD150⁺CD48⁻LSKs; Fig. 5G) in total spleen MNCs. While we did not observe any change in the HSPC population (Suppl. Fig. 3B), there was a significant increase in the frequency of LSK cells (Fig. 5F) and primitive HSCs (Fig. 5G). We then asked if this increase in the stem cell frequency was linked to altered proliferation status (Fig. 5H,I). The LSK population was analyzed for cell cycle status using Hoechst 33342 and Pyronin Y staining (Fig. 5H, gated on LSK cells). Although we did not observe any significant change in the proportion of quiescent LSK cells (G0 stage), we observed a decrease in the cells in G1 (from 33.18±2.05% to 25.46±2.59%; Fig. 5I). Concomitantly, we found increase in the proportion of cells in S (from 9.16±1.60% to 15.52±1.31%) as well as G2/M phase (from 8.79±1.25% to 13.07±0.87%) of cell cycle. These results demonstrate faster proliferation of the spleen resident hematopoietic progenitors, as observed in the case of *Vav-Itgav*^{-/-} mice.

Through careful histological analyses, we observed that *Postn* deletion led to an increase in the trabecular area (Fig. 6A,B). In addition, as in the case of *Vav-Itgav*^{-/-} mice, we observed a significant increase in the RP area (Fig. 6C; Suppl. Fig. 3C), with a corresponding decrease in the WP area (Fig. 6C, Suppl. Fig. 3D) resulting in overall increase in the RP/WP ratio (Fig. 6D). However, *Postn* deletion did not result in any change in the proportion of myeloid (CD11b/Gr-1⁺; Suppl. Fig. 3E), T-(CD4/CD8⁺; Suppl. Fig. 3F), or B- cell (B220⁺; Suppl. Fig. 3G) populations. Flow cytometry analysis also showed a significant increase in the proportion of CD41⁺ cells in the spleen MNC population (Suppl. Fig. 3H). In order to confirm that the increase in CD41⁺ cells indicated a rise in the megakaryocytic population, we performed H&E staining and compared the density of megakaryocytes, identified based on their morphology (number per unit area) and confirmed increase in the megakaryocyte population (Fig. 6E,F).

POSTN deficient spleen provides poor support to transplanted HSCs

Integrins are known for their role in cellular attachment in several cell types, including the hematopoietic system. Our studies published before, did not find any difference in the adhesion of *Itgav* deficient HSCs *in vitro*, also reflected in their homing potential *in vivo* (12, 30). Therefore, we examined if there was any mobilization of BM HSPCs that could aid in splenic extramedullary hematopoietic activity. Peripheral blood borne hematopoietic progenitors in *Postn*^{+/+} versus *Postn*^{-/-} mice were quantified using CFU-C assays (Fig. 6G). We did not find any significant increase in the circulating hematopoietic progenitors in mice lacking POSTN expression. These results indicated that the phenotypes observed were due to spleen-intrinsic effects of *Postn* deletion. Next, we examined if hematopoietic stress condition further impacted the HSPC population in spleen. We used sub-lethal dose of radiation to inflict hematopoietic injury and assessed the impact on the splenic HSPC population in *Postn*^{+/+} versus *Postn*^{-/-} mice using methylcellulose-based colony assays (Fig. 6H). As expected, we observed a decrease in the number of splenic CFU-Cs following radiation in both the groups. However, the radiation induced decrease in CFU-Cs was significantly more pronounced in *Postn*-deficient mice. We hypothesized that these effects might be due to poor support for the HSPC function in splenic niche lacking POSTN. To confirm this, we tested if there was any change in niche support for the incoming HSCs following BM transplantation in irradiated mice. We performed colony forming unit-spleen assay (CFU-S₁₂), wherein we transplanted healthy BM derived cells into WT (*Postn*^{+/+}) or KO (*Postn*^{-/-}) mice and compared the number of spleen colonies formed after 12 days (Fig. 6I,J). We normalized the number of colonies formed with the weight of the spleens and observed a significantly decreased number of spleen colonies in KO mice after 12 days of transplantation (Fig. 6K). We also compared the frequency of HSC sub-populations in the spleen tissues in the mice by flow cytometry analysis (Fig. 6L-N). While we observed a significant decrease in the frequency of lin⁻c-kit⁺ hematopoietic progenitors (Fig. 6L) and LSK cells (Fig. 6M), there was no difference in the frequency of the primitive HSCs (Fig. 6N). We did not observe any difference in the frequency of the lin⁻c-kit⁺ (Suppl. Fig. 3I), LSK cells (Suppl. Fig. 3J) and the primitive HSC populations (Suppl. Fig. 3K) of the BM. These results indicate that POSTN deficient spleen microenvironment might be poorer in its potential to maintain incoming hematopoietic progenitors.

Discussion

We here present evidence for a role of POSTN-ITGAV interaction in spleen lymphohematopoietic activity. Interruption in this interaction in *Postn*^{-/-} as well as *Vav-Itgav*^{-/-} led to increased proliferation rates in spleen HSC population. The impact of altered inside-out integrin signaling has been reported to affect spleen hematopoiesis through mobilization of hematopoietic progenitors due to altered BM hematopoietic niche (33). These effects could also be linked to poor homing of HSCs during embryonic development (34). Although, yolk sac (YS) did show the presence of *Itgb1*^{-/-} HSCs in the chimeric mice, they were not detected in embryonic blood or the hematopoietic sites including spleen. Later, Alexander Medvinsky's group through a comprehensive study showed that ITGA4, a key partner in integrin heterodimers with $\beta 1$ chain, was not crucial for differentiation program in definitive HSCs (35). Furthermore, Talin1 that mediates association between integrin chains to actin cytoskeleton for cellular adhesion, was also shown to be dispensable for follicular B-cell maturation in spleen (36). While these and several other studies explored the role of inside-out integrin signaling in hematopoiesis, a role of outside-in integrin signaling in spleen hematopoietic function has not been characterized yet. In corroboration of our previous studies, we observed increased rate of HSC proliferation in both *Postn*^{-/-} and *Vav-Itgav*^{-/-} spleen. Importantly, methylcellulose-based colony assays showed a clear decline in their multi-lineage differentiation potential as fewer CFU-GEMMs were observed in *Vav-Itgav*^{-/-} spleen, despite an increase in the frequency of LSK and CD150⁺CD48⁻LSK cells.

It has been previously shown through *in vitro* experiments that POSTN plays a role in B-lymphopoiesis (37). Our previous study showed a decrease in the number of lymphocytes in PB of *Postn* deficient mice (12). The experiments presented in this study, clearly showed a decrease in the WP area indicating an effect on lymphopoietic activity. Flow cytometry experiments confirmed a B-cell specific effect upon *Vav-iCre* mediated loss of *Itgav*. Apart from an increase in the RP/WP ratio and a modest increase in overall spleen size, there was no indication of extramedullary hematopoiesis. Both *Postn*^{-/-} and *Vav-Itgav*^{-/-} mice showed increase in megakaryocyte numbers. In fact, there was a remarkable similarity in the phenotype of the two mouse lines used in this study. This, despite the fact that there are other known ligands for integrin heterodimers with ITGAV as one of the components. Although, integrins with ITGAV chain have been shown to act as the common receptors for POSTN (38), it has been shown to have binding affinity for other integrin heterodimers, such as ITGAM-B2, as well (39). A number of terminally differentiated blood cells, such as macrophages and monocytes express ITGAM-B2 (40). A direct effect of loss of POSTN on their function cannot be ruled out, but our results show a clear alteration in the function of hematopoietic stem and progenitor cell population upon the loss of POSTN-ITGAV interaction. Moreover, largely overlapping splenic phenotype seen in *Postn*^{-/-} and *Vav-Itgav*^{-/-} mice also indicates the importance of their association. Several ECM proteins, soluble factors as well as ECM binding proteins such as Osteopontin (OPN) have been shown to bind heterodimers containing ITGAV (41). OPN is an established negative regulator of HSC function and *Opn*^{-/-} mice showed increased numbers of HSCs in the BM as well as spleen (16). Under pathological conditions, soluble isoform of OPN increased lymphoid cell population in BM chimeras (42). In our earlier published

work, *Vav-iCre* mediated deletion of *Itgav* led to decline in HSC function with increased proliferation rates. Our recent studies on fetal liver hematopoiesis also showed increase in HSC proliferation rates both in the case of *Postn*^{-/-} and *Vav-Itgav*^{-/-} embryos (30). Through the results presented in this manuscript, we further establish the role of POSTN-ITGAV interaction in the regulation of HSC proliferation.

We made another curious observation on spleen tissues from *Postn* deficient mice. The tissue showed an increase in the trabecular area. We did not observe this phenotype in *Vav-Itgav*^{-/-} spleen and hypothesized the presence of an additional hematopoietic-extrinsic effect of loss of *Postn*. This was corroborated by an overall small size of *Postn* deficient spleen, unlike in the case of *Vav-iCre* mediated *Itgav* deletion. Further proof came from CFU-S₁₂ assay, wherein transplanted WT BM cells were poorly supported by the *Postn* deficient spleen niche and resulted in fewer spleen colonies. It is interesting to note that we observed POSTN expression mainly in the myofibroblasts of spleen trabeculae. It has been shown before that POSTN is expressed in myofibroblasts in a variety of tissues including skin (43). In fact, *Postn*-gene targeted mouse line was raised to delineate the developmental origin of myofibroblasts in cardiac tissue (44). Increase in the trabecular area in *Postn* deficient mice points towards a feedback regulatory mechanism connecting POSTN expression and function. These observations warrant further investigation into the role of POSTN in the creation of splenic niche and its impact on the non-hematopoietic compartment of the tissue. *Vav-iCre* mediated transgenesis targets cells of endothelial and hematopoietic origin (45) not affecting the other cell types such as mesenchymal cells and myofibroblasts. Therefore, phenotypic differences between the *Postn*^{-/-} and *Vav-Itgav*^{-/-} mice, including overall decrease in spleen size in *Postn*^{-/-} mice, is not unexpected. In fact, expansion of the trabecular area that is also the key source of POSTN expression and secretion, indicates a possible autocrine regulation. Poorer support for the incoming hematopoietic progenitors HSCs observed through CFU-S₁₂ assays could also have resulted due to altered physico-structural support from the spleen niche in *Postn*^{-/-} mice. Further studies could shed light on many of the pathological conditions that lead to fibrous splenic areas (46).

Niche regulation of spleen resident HSCs has not been worked out yet. Using extramedullary hematopoiesis model, Sean Morrison's group through elegant experiments showed the involvement of *Tcf21*-expressing endothelial and stromal cells in supporting HSCs in spleen (47). HSCs were found to be located close to the *Tcf21*⁺ stromal cells in the red pulp of spleen. These cells expressed SCF and SDF-1 α ; conditional deletion of anyone of these two genes, resulted in severely reduced spleen EMH. Potential of spleen stroma to support hematopoietic activity through *in vitro* experiments had been described (48). These cells supported the lymphoid cells from BM, spleen, thymus and blood in secondary cultures and led to robust differentiation into dendritic cells. Spleen stromal cell lines were later established that showed potential to support the development of hematopoietic cells including immature dendritic-like cells (49). Recently, these stromal cells that showed a rather restricted support of hematopoietic processes were found to be equivalent to Sca-1⁺gp38⁺Thy1.2⁺CD29⁺CD51⁺ fraction of spleen stroma (50). However, mechanisms that regulate the function of spleen resident HSCs have not been uncovered thus far. Associated phenotype of increased trabecular area in spleen from *Postn*^{-/-} mice indicates a possible regulation by the physical components of the niche. Further investigation could

also be important to understand spleen fibrotic pathologies better. In the case of liver cirrhosis, it has been shown that transforming growth factor (TGF)- β expressed in spleen plays an important role (51). While TGF- β is known to be an important regulator of *Postn* expression (52), a number of POSTN-induced functions, such as collagen production, were mediated by TGF- β (53). In our experiments however, we did not observe any significant change in *Tgf- β 1* expression in *Postn* deficient spleen tissue (data not shown).

As there was no induction of EMH upon *Postn*-deletion, we considered that the phenotypes observed were mediated via the effects on spleen resident HSCs. Although their physiological relevance in the regular supply of blood cells or even EMH is not clearly understood, at clonal level their in vivo function was found to be equivalent to that of the BM HSCs (22). It has been reported that suppression of BM hematopoiesis is not crucial for the induction of EMH and extrinsic factors could stimulate increase in the number of hematopoietic progenitors in spleen and liver (54). A double transgenic mouse co-expressing IL-6 and soluble IL-6R showed elevated levels of EMH in spleen in addition to liver, without impacting BM hematopoiesis. IL-6 is a well-known player in inflammation and various related immunological responses (55). Work in the recent years has elucidated a clear effect of infections and inflammation in affecting HSC function (56, 57). However, if IL-6 mediated any of these effects is not very clear. Spleen function is more intricately connected with the immunological status of the organisms. A recent report suggested regulation of IL-6 expression by POSTN, as in the *Postn*^{-/-} colonic tissues IL-6 expression was found to be reduced. Interestingly, IL-6 in turn induced STAT3 mediated *Postn* expression in colonic myofibroblasts (58). Similar findings were made in the case of keratinocyte proliferation where POSTN regulated its own expression through a IL-1 α /IL-6 loop (59). As IL-6 also, is a known regulator of collagen (60), its role on mediating some of the phenotypes observed in *Postn*^{-/-} mice could not be ruled out.

In contrast, *hck*^{-/-}*Src*^{-/-} mice showed activation of EMH followed by severely affected BM hematopoiesis due to extreme form of osteopetrosis (61). Therefore, it has been challenging to understand the regulatory mechanisms that are played specifically in the spleen and their physiological relevance. Our report shows the involvement of outside-in integrin signaling not only in the regulation of spleen HSC function but possibly also in the creation of hematopoietic niche in this tissue.

Supplementary Material

Refer to Web version on PubMed Central for supplementary material.

Acknowledgement

The authors wish to thank Dr. Adam Lacy-Hulbert for providing *Itgav*^{f1/f1} mice used in this work.

Grant Support

This work was supported by the Wellcome Trust/DBT India Alliance Fellowship (IA/I/15/2/502061) awarded to SK and intramural funds from Indian Institute of Science Education and Research Thiruvananthapuram (IISER TVM). Institutional animal facility is supported by funds from the Department of Science and Technology, Government of India (under FIST scheme; SR/FST/LS-II/2018/217). SHM and AB are supported by IISER TVM. IMR is supported by Senior Research Fellowship from University Grants Commission (UGC), India. DP received

support from INSPIRE fellowship from DST, India. CMV is supported by funds from KU Leuven (IDO/13/016 HSC-Niche) and FWO (G0E0117N).

References

1. Hoggatt J, Kfoury Y, Scadden DT. Hematopoietic Stem Cell Niche in Health and Disease. *Annu Rev Pathol.* 2016; 11 :555–581. [PubMed: 27193455]
2. Mebius RE, Kraal G. Structure and function of the spleen. *Nat Rev Immunol.* 2005; 5 :606–616. [PubMed: 16056254]
3. Wolber FM, Leonard E, Michael S, Orschell-Traycoff CM, Yoder MC, Srour EF. Roles of spleen and liver in development of the murine hematopoietic system. *Experimental hematology.* 2002; 30 :1010–1019. [PubMed: 12225792]
4. Yamamoto K, Miwa Y, Abe-Suzuki S, Abe S, Kirimura S, Onishi I, Kitagawa M, Kurata M. Extramedullary hematopoiesis: Elucidating the function of the hematopoietic stem cell niche. *Mol Med Rep.* 2016; 13 :587–591. [PubMed: 26648325]
5. Johns JL, Christopher MM. Extramedullary hematopoiesis: a new look at the underlying stem cell niche, theories of development, and occurrence in animals. *Vet Pathol.* 2012; 49 :508–523. [PubMed: 22262354]
6. Dutta P, Hoyer FF, Grigoryeva LS, Sager HB, Leuschner F, Courties G, Borodovsky A, Novobrantseva T, Ruda VM, Fitzgerald K, Iwamoto Y, et al. Macrophages retain hematopoietic stem cells in the spleen via VCAM-1. *The Journal of experimental medicine.* 2015; 212 :497–512. [PubMed: 25800955]
7. Alon R, Kassner PD, Carr MW, Finger EB, Hemler ME, Springer TA. The integrin VLA-4 supports tethering and rolling in flow on VCAM-1. *The Journal of cell biology.* 1995; 128 :1243–1253. [PubMed: 7534768]
8. Williams DA, Rios M, Stephens C, Patel VP. Fibronectin and VLA-4 in haematopoietic stem cell-microenvironment interactions. *Nature.* 1991; 352 :438–441. [PubMed: 1861722]
9. Ramirez P, Rettig MP, Uy GL, Deych E, Holt MS, Ritchey JK, DiPersio JF. BIO5192, a small molecule inhibitor of VLA-4, mobilizes hematopoietic stem and progenitor cells. *Blood.* 2009; 114 :1340–1343. [PubMed: 19571319]
10. Craddock CF, Nakamoto B, Andrews RG, Priestley GV, Papayannopoulou T. Antibodies to VLA4 integrin mobilize long-term repopulating cells and augment cytokine-induced mobilization in primates and mice. *Blood.* 1997; 90 :4779–4788. [PubMed: 9389694]
11. Prosper F, Verfaillie CM. Regulation of hematopoiesis through adhesion receptors. *Journal of leukocyte biology.* 2001; 69 :307–316. [PubMed: 11261776]
12. Khurana S, Schouteden S, Manesia JK, Santamaria-Martinez A, Huelsken J, LacyHulbert A, Verfaillie CM. Outside-in integrin signalling regulates haematopoietic stem cell function via Periostin-Itgav axis. *Nature communications.* 2016; 7 13500
13. Papayannopoulou T, Craddock C, Nakamoto B, Priestley GV, Wolf NS. The VLA4/VCAM-1 adhesion pathway defines contrasting mechanisms of lodgement of transplanted murine hemopoietic progenitors between bone marrow and spleen. *Proceedings of the National Academy of Sciences of the United States of America.* 1995; 92 :9647–9651. [PubMed: 7568190]
14. Potocnik AJ, Brakebusch C, Fassler R. Fetal and adult hematopoietic stem cells require beta1 integrin function for colonizing fetal liver, spleen, and bone marrow. *Immunity.* 2000; 12 :653–663. [PubMed: 10894165]
15. Nilsson SK, Johnston HM, Whitty GA, Williams B, Webb RJ, Denhardt DT, Bertoncello I, Bendall LJ, Simmons PJ, Haylock DN. Osteopontin, a key component of the hematopoietic stem cell niche and regulator of primitive hematopoietic progenitor cells. *Blood.* 2005; 106 :1232–1239. [PubMed: 15845900]
16. Stier S, Ko Y, Forkert R, Lutz C, Neuhaus T, Grunewald E, Cheng T, Dombkowski D, Calvi LM, Rittling SR, Scadden DT. Osteopontin is a hematopoietic stem cell niche component that negatively regulates stem cell pool size. *The Journal of experimental medicine.* 2005; 201 :1781–1791. [PubMed: 15928197]

17. Wai PY, Kuo PC. Osteopontin: regulation in tumor metastasis. *Cancer Metastasis Rev.* 2008; 27 :103–118. [PubMed: 18049863]
18. Izuhara K, Nunomura S, Nanri Y, Ogawa M, Ono J, Mitamura Y, Yoshihara T. Periostin in inflammation and allergy. *Cellular and Molecular Life Sciences.* 2017; 74 :4293–4303. [PubMed: 28887633]
19. Umemoto T, Matsuzaki Y, Shiratsuchi Y, Hashimoto M, Yoshimoto T, Nakamura-Ishizu A, Petrich B, Yamato M, Suda T. Integrin alpha v beta 3 enhances the suppressive effect of interferon-gamma on hematopoietic stem cells. *Embo Journal.* 2017; 36 :2390–2403.
20. Acharya M, Mukhopadhyay S, Paidassi H, Jamil T, Chow C, Kissler S, Stuart LM, Hynes RO, Lacy-Hulbert A. alphav Integrin expression by DCs is required for Th17 cell differentiation and development of experimental autoimmune encephalomyelitis in mice. *The Journal of clinical investigation.* 2010; 120 :4445–4452. [PubMed: 21099114]
21. Masuoka M, Shiraishi H, Ohta S, Suzuki S, Arima K, Aoki S, Toda S, Inagaki N, Kurihara Y, Hayashida S, Takeuchi S, et al. Periostin promotes chronic allergic inflammation in response to Th2 cytokines. *Journal of Clinical Investigation.* 2012; 122 :2590–2600.
22. Morita Y, Iseki A, Okamura S, Suzuki S, Nakauchi H, Ema H. Functional characterization of hematopoietic stem cells in the spleen. *Experimental hematology.* 2011; 39 :351–359. e353 [PubMed: 21185906]
23. Malanchi I, Santamaria-Martinez A, Susanto E, Peng H, Lehr HA, Delaloye JF, Huelsken J. Interactions between cancer stem cells and their niche govern metastatic colonization. *Nature.* 2012; 481 :85–89.
24. Lacy-Hulbert A, Smith AM, Tissire H, Barry M, Crowley D, Bronson RT, Roes JT, Savill JS, Hynes RO. Ulcerative colitis and autoimmunity induced by loss of myeloid alphav integrins. *Proc Natl Acad Sci U S A.* 2007; 104 :15823–15828. [PubMed: 17895374]
25. de Boer J, Williams A, Skavdis G, Harker N, Coles M, Tolaini M, Norton T, Williams K, Roderick K, Potocnik AJ, Kioussis D. Transgenic mice with hematopoietic and lymphoid specific expression of Cre. *Eur J Immunol.* 2003; 33 :314–325. [PubMed: 12548562]
26. Arai F, Hirao A, Ohmura M, Sato H, Matsuoka S, Takubo K, Ito K, Koh GY, Suda Y. Tie2/angiopoietin-1 signaling regulates hematopoietic stem cell quiescence in the bone marrow niche. *Cell.* 2004; 118 :149–161. [PubMed: 15260986]
27. Till JE, Mc CE. A direct measurement of the radiation sensitivity of normal mouse bone marrow cells. *Radiat Res.* 1961; 14 :213–222. [PubMed: 13776896]
28. Phillips R, Svensson M, Aziz N, Maroof A, Brown N, Beattie L, Signoret N, Kaye PM. Innate killing of *Leishmania donovani* by macrophages of the splenic marginal zone requires IRF-7. *PLoS Pathog.* 2010; 6 e1000813 [PubMed: 20300600]
29. Martinez-Pomares L, Gordon S. CD169(+) macrophages at the crossroads of antigen presentation. *Trends Immunol.* 2012; 33 :66–70. [PubMed: 22192781]
30. Biswas A, Roy IM, Babu PC, Manesia J, Schouteden S, Vijayakurup V, Anto RJ, Huelsken J, Lacy-Hulbert A, Verfaillie CM, Khurana S. The Periostin/Integrin-alphav Axis Regulates the Size of Hematopoietic Stem Cell Pool in the Fetal Liver. *Stem Cell Reports.* 2020
31. Savill J, Dransfield I, Hogg N, Haslett C. Vitronectin receptor-mediated phagocytosis of cells undergoing apoptosis. *Nature.* 1990; 343 :170–173. [PubMed: 1688647]
32. Eliceiri BP, Cheresh DA. Adhesion events in angiogenesis. *Current opinion in cell biology.* 2001; 13 :563–568. [PubMed: 11544024]
33. Scott LM, Priestley GV, Papayannopoulou T. Deletion of alpha4 integrins from adult hematopoietic cells reveals roles in homeostasis, regeneration, and homing. *Mol Cell Biol.* 2003; 23 :9349–9360. [PubMed: 14645544]
34. Hirsch E, Iglesias A, Potocnik AJ, Hartmann U, Fassler R. Impaired migration but not differentiation of haematopoietic stem cells in the absence of beta(1) integrins. *Nature.* 1996; 380 :171–175. [PubMed: 8600394]
35. Gribi R, Hook L, Ure J, Medvinsky A. The differentiation program of embryonic definitive hematopoietic stem cells is largely alpha4 integrin independent. *Blood.* 2006; 108 :501–509. [PubMed: 16551970]

36. Manevich-Mendelson E, Grabovsky V, Feigelson SW, Cinamon G, Gore Y, Goverse G, Monkley SJ, Margalit R, Melamed D, Mebius RE, Critchley DR, et al. Talin1 is required for integrin-dependent B lymphocyte homing to lymph nodes and the bone marrow but not for follicular B-cell maturation in the spleen. *Blood*. 2010; 116 :5907–5918. [PubMed: 20923969]
37. Siewe BT, Kalis SL, Le PT, Witte PL, Choi S, Conway SJ, Druschitz L, Knight KL. In vitro requirement for periostin in B lymphopoiesis. *Blood*. 2011; 117 :3770–3779. [PubMed: 21285437]
38. Gillan L, Matei D, Fishman DA, Gerbin CS, Karlan BY, Chang DD. Periostin secreted by epithelial ovarian carcinoma is a ligand for alpha(V)beta(3) and alpha(V)beta(5) integrins and promotes cell motility. *Cancer Res*. 2002; 62 :5358–5364. [PubMed: 12235007]
39. Johansson MW, Annis DS, Mosher DF. Alphabeta2 Integrin-Mediated Adhesion And Motility Of Interleukin-5-Stimulated Eosinophils On Periostin. *Am J Resp Crit Care*. 2013; 187
40. Fan ST, Edgington TS. Coupling of the Adhesive Receptor Cd11b/Cd18 to Functional Enhancement of Effector Macrophage Tissue Factor Response. *Journal of Clinical Investigation*. 1991; 87 :50–57.
41. Ross FP, Chappel J, Alvarez JI, Sander D, Butler WT, Farach-Carson MC, Mintz KA, Robey PG, Teitelbaum SL, Cheresh DA. Interactions between the bone matrix proteins osteopontin and bone sialoprotein and the osteoclast integrin alpha v beta 3 potentiate bone resorption. *J Biol Chem*. 1993; 268 :9901–9907. [PubMed: 8486670]
42. Kanayama M, Xu S, Danzaki K, Gibson JR, Inoue M, Gregory SG, Shinohara ML. Skewing of the population balance of lymphoid and myeloid cells by secreted and intracellular osteopontin. *Nat Immunol*. 2017; 18 :973–984. [PubMed: 28671690]
43. Zhou HM, Wang J, Elliott C, Wen WY, Hamilton DW, Conway SJ. Spatiotemporal expression of periostin during skin development and incisional wound healing: lessons for human fibrotic scar formation. *J Cell Commun Signal*. 2010; 4 :99–107. [PubMed: 20531985]
44. Kanisicak O, Khalil H, Ivey MJ, Karch J, Maliken BD, Correll RN, Brody MJ, Lin SCJ, Aronow BJ, Tallquist MD, Molkentin JD. Genetic lineage tracing defines myofibroblast origin and function in the injured heart. *Nature communications*. 2016; 7
45. Joseph C, Quach JM, Walkley CR, Lane SW, Lo Celso C, Purton LE. Deciphering hematopoietic stem cells in their niches: a critical appraisal of genetic models, lineage tracing, and imaging strategies. *Cell stem cell*. 2013; 13 :520–533. [PubMed: 24209759]
46. Kondo R, Kage M, Iijima H, Fujimoto J, Nishimura T, Aizawa N, Akiba J, Naito Y, Kusano H, Nakayama M, Mihara Y, et al. Pathological findings that contribute to tissue stiffness in the spleen of liver cirrhosis patients. *Hepato Res*. 2018; 48 :1000–1007. [PubMed: 29766631]
47. Inra CN, Zhou BO, Acar M, Murphy MM, Richardson J, Zhao Z, Morrison SJ. A perisinusoidal niche for extramedullary haematopoiesis in the spleen. *Nature*. 2015; 527 :466–471. [PubMed: 26570997]
48. Ni K, O'Neill H. Spleen stromal cells support haemopoiesis and in vitro growth of dendritic cells from bone marrow. *Br J Haematol*. 1999; 105 :58–67. [PubMed: 10233363]
49. Periasamy P, Tan JK, Griffiths KL, O'Neill HC. Splenic stromal niches support hematopoiesis of dendritic-like cells from precursors in bone marrow and spleen. *Experimental hematology*. 2009; 37 :1060–1071. [PubMed: 19539692]
50. Lim HK, O'Neill HC. Identification of Stromal Cells in Spleen Which Support Myelopoiesis. *Front Cell Dev Biol*. 2019; 7 (1)
51. Akahoshi T, Hashizume M, Tanoue K, Shimabukuro R, Gotoh N, Tomikawa M, Sugimachi K. Role of the spleen in liver fibrosis in rats may be mediated by transforming growth factor beta-1. *J Gastroen Hepatol*. 2002; 17 :59–65.
52. Horiuchi K, Amizuka N, Takeshita S, Takamatsu H, Katsuura M, Ozawa H, Toyama Y, Bonewald LF, Kudo A. Identification and characterization of a novel protein, periostin, with restricted expression to periosteum and periodontal ligament and increased expression by transforming growth factor beta. *J Bone Miner Res*. 1999; 14 :1239–1249. [PubMed: 10404027]
53. Sidhu SS, Yuan SP, Innes AL, Kerr S, Woodruff PG, Hou L, Muller SJ, Fahy JV. Roles of epithelial cell-derived periostin in TGF-beta activation, collagen production, and collagen gel elasticity in asthma. *Proceedings of the National Academy of Sciences of the United States of America*. 2010; 107 :14170–14175. [PubMed: 20660732]

54. Peters M, Schirmacher P, Goldschmitt J, Odenthal M, Peschel C, Fattori E, Ciliberto G, Dienes HP, Meyer zum Buschenfelde KH, Rose-John S. Extramedullary expansion of hematopoietic progenitor cells in interleukin (IL)-6-sIL-6R double transgenic mice. *The Journal of experimental medicine*. 1997; 185 :755–766. [PubMed: 9034153]
55. Tanaka T, Narazaki M, Kishimoto T. IL-6 in Inflammation, Immunity, and Disease. *Csh Perspect Biol*. 2014; 6
56. Takizawa H, Regoes RR, Boddupalli CS, Bonhoeffer S, Manz MG. Dynamic variation in cycling of hematopoietic stem cells in steady state and inflammation. *Journal of Experimental Medicine*. 2011; 208 :273–284.
57. Pietras EM. Inflammation: a key regulator of hematopoietic stem cell fate in health and disease. *Blood*. 2017; 130 :1693–1698. [PubMed: 28874349]
58. Ma HD, Wang J, Zhao XL, Wu TT, Huang ZJ, Chen DF, Liu YF, Ouyang GL. Periostin Promotes Colorectal Tumorigenesis through Integrin-FAK-Src Pathway-Mediated YAP/TAZ Activation. *Cell Reports*. 2020; 30 :793. [PubMed: 31968254]
59. Taniguchi K, Arima K, Masuoka M, Ohta S, Shiraishi H, Ohtsuka K, Suzuki S, Inamitsu M, Yamamoto K, Simmons O, Toda S, et al. Periostin Controls Keratinocyte Proliferation and Differentiation by Interacting with the Paracrine IL-1 alpha/IL-6 Loop. *Journal of Investigative Dermatology*. 2014; 134 :1295–1304.
60. Duncan MR, Berman B. Stimulation of Collagen and Glycosaminoglycan Production in Cultured Human Adult Dermal Fibroblasts by Recombinant Human Interleukin-6. *Journal of Investigative Dermatology*. 1991; 97 :686–692.
61. Lowell CA, Niwa M, Soriano P, Varmus HE. Deficiency of the Hck and Src tyrosine kinases results in extreme levels of extramedullary hematopoiesis. *Blood*. 1996; 87 :1780–1792. [PubMed: 8634424]

Key points

- Outside-in integrin signaling regulates splenic HSC proliferation and function.
- Lack of Postn-Itgav interaction affects myofibroblasts in splenic trabecular area.
- Periostin modulates splenic niche creation and support for splenic and incoming HSCs.

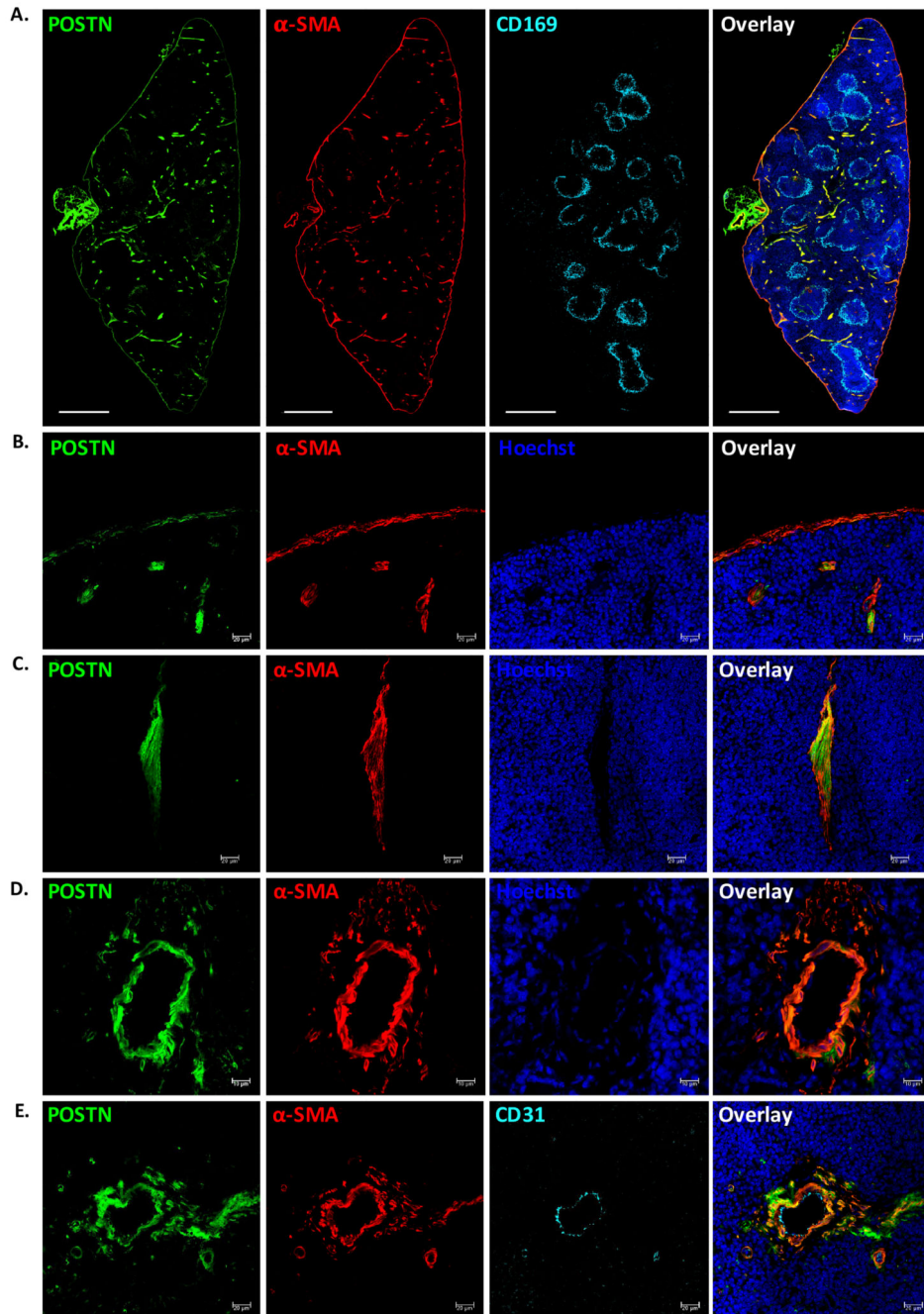


Figure 1. POSTN is expressed by myofibroblasts in adult spleen

(A) POSTN expression in adult spleen tissues was examined using immunohistochemistry on 10 μ m cryo-sections. WP areas were identified by using marginal zone macrophage marker CD169; trabecular, capsular and vascular regions were identified by using antibodies against α -SMA. Specific antibodies were used to identify the cells expressing POSTN, nuclear counterstaining was done using Hoechst 33342. The sections were visualized and tile scan was performed on confocal microscopes. (n=2, N=8, scale bar=0.5mm).

(B-D) Regions with compelling levels of POSTN expression; namely, the capsule (B), trabeculae (C), and vasculature (D) were analyzed by immunostaining with myofibroblast/smooth muscle cell marker α -SMA. (n=5, scale bar= 20 μ m for panel B,C and 10 μ m for panel D).

(E) The endothelial and smooth muscle lining of the vessels were identified using antibodies against endothelial marker CD31 and α -SMA, along with anti-POSTN antibody (n=3, scale bar=20 μ m).

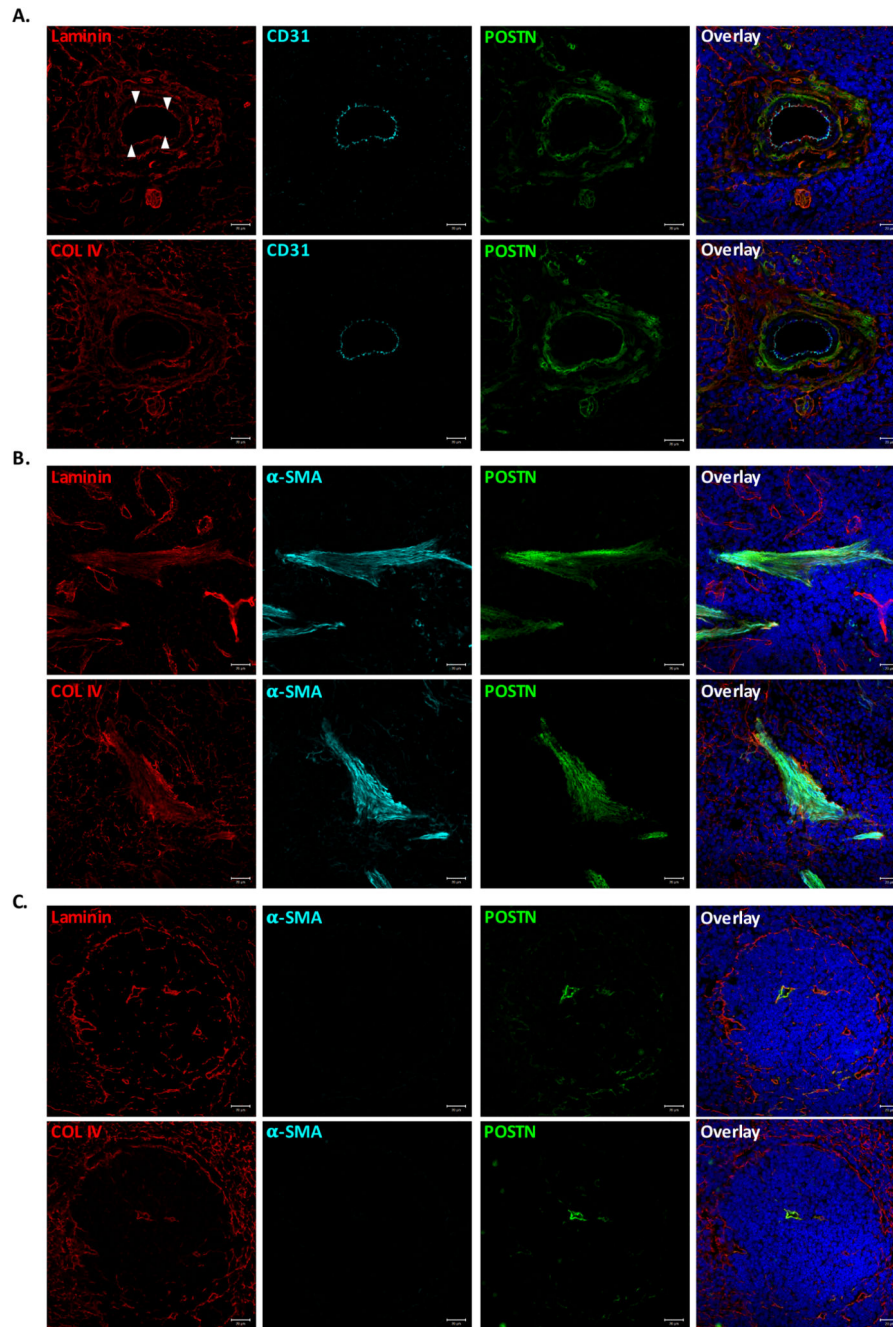


Figure 2. POSTN colocalizes with ECM proteins close to myofibroblasts

Immunostaining experiments were performed to examine colocalization of POSTN with ECM proteins laminin and collagen IV in various anatomical locations within spleen tissue. (A) Vascular region of spleen identified by CD31 immunostaining. Colocalization of POSTN with laminin (upper panel) and collagen IV (lower panel) visualized using specific antibodies. (B) Staining for α -SMA was used to identify trabecular area, wherein POSTN colocalization with ECM was examined by counterstaining with laminin (upper panel) and collagen IV (lower panel). (C) White pulp area, identified by the laminin (upper panel) and

collagen IV (lower panel) expression on the periphery and in red pulp. Identification of smooth muscle cells/myofibroblasts and POSTN using specific antibodies.
n=3, Scale bar=20 μ m

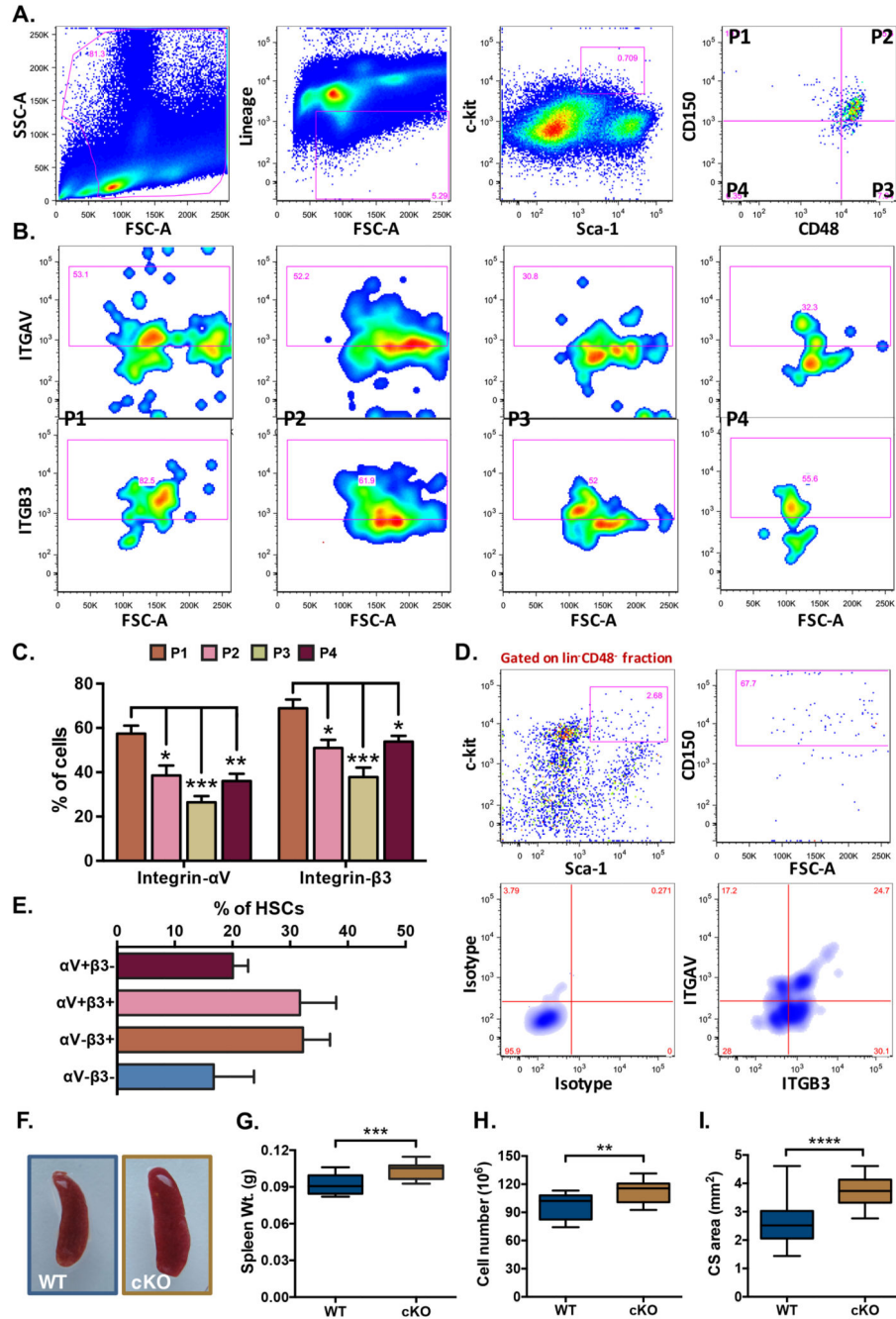


Figure 3. Expression of ITGAV and ITGB3 in hematopoietic stem cell sub-populations in spleen
 Adult spleen derived MNCs were analyzed for the cell surface expression of ITGAV and ITGB3 on various HSC sub-populations by flow cytometry. (A) The LSK population from the spleen MNCs was further divided into four sub-populations on the basis of expression of SLAM markers CD150 and CD48. (B) All four sub-populations of the LSK cells were examined for the expression of ITGAV (upper panel) and ITGB3 (lower panel), separately. (C) Comparison of ITGAV and ITGB3 expression on different HSC sub-populations. Proportion of each LSK sub-population based on CD150 and CD48 that

expressed ITGAV or ITGB3 was plotted. One-way ANOVA followed by Tukey-Kramer Post Hoc test was performed * $p < 0.05$, ** $p < 0.01$. (D) Co-expression analysis of ITGAV and ITGB3 on the primitive HSCs. The adult spleen derived HSCs were identified as $\text{lin}^- \text{CD48}^- \text{c-kit}^+ \text{Sca-1}^+ \text{CD150}^+$ cells and were examined for the expression of ITGAV and ITGB3 based on flow cytometry. (E) Proportion of primitive HSCs expressing ITGAV and ITGB3 in combination or separately. (F) Gross morphology of the spleen from *Vav-Itgav*^{+/+} (WT) and *Vav-Itgav*^{-/-} (conditional knockout; cKO) mice obtained following crossing *Vav-iCre* and *Itgav*^{fl/fl} lines. (G) Comparison of whole spleen weight from WT and cKO mice. (H) Comparison of total spleen cellularity (total mononuclear cells) in the WT and cKO mice. (I) Cross-sectional area quantified using transverse sections through the spleen tissues. Six 10 μm thick sections (every fifth section used for analysis), were analyzed for total cross-sectional area. $n=4$, $N=24$, * $p < 0.05$, ** $p < 0.01$, *** $p < 0.001$, **** $p < 0.0001$, ns indicates not significant.

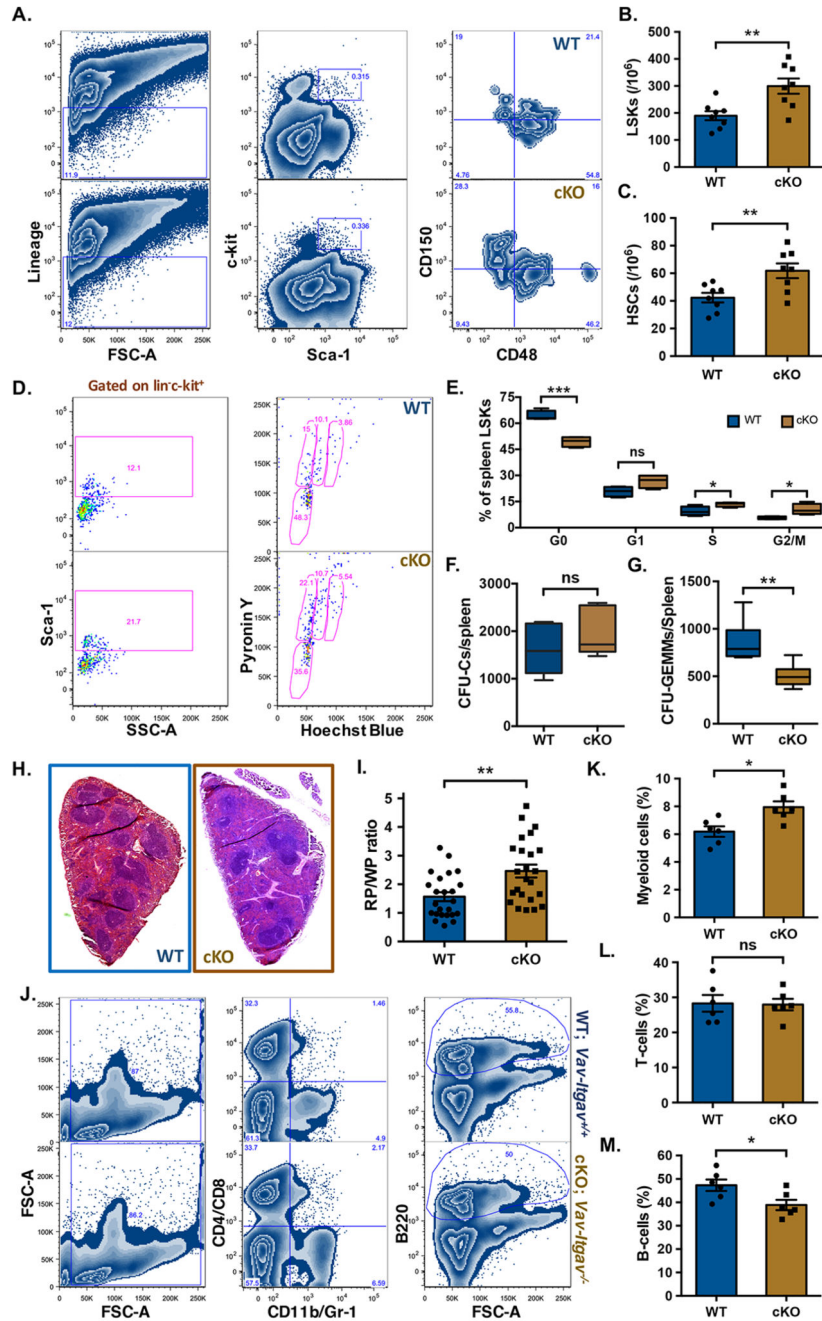


Figure 4. Increased frequency of phenotypic HSCs and poor B-lymphopoiesis in *Vav-Itgav^{-/-}* spleen

(A-C) Mononuclear cells from *Vav-Itgav^{+/+}* (WT), *Vav-Itgav^{-/-}* (cKO) spleen tissues were used for the analysis of HSC frequency by flow cytometry. Quantification of frequency of hematopoietic stem and progenitor cell populations in the spleen from WT and cKO mice; (A) The LSK population from the spleen MNCs was further divided on the basis of expression of SLAM markers CD150 and CD48, (B) LSK cells, (C) primitive HSCs (n=8). (D,E) Cell cycle analysis of the primitive HSCs population from spleen by Hoechst 33342/Pylonin Y staining. Comparison of the proportion of spleen LSK cells in various

stages of cell cycle is shown (n=6). (F,G) CFU-C assay performed on total splenocytes to compare the frequency of hematopoietic progenitors. Total number of CFU-Cs (F) and CFU-GEMMs (G) were compared between WT and cKO mice (n=6). (H) Spleen tissues from *Vav-Itgav^{+/+}* (WT) and *Vav-Itgav^{-/-}* (cKO) animals were harvested. The formalin-fixed, paraffin-embedded tissues were used to cut 10 μ m sections that were used for H&E staining. (I) The ratio between the cross-sectional area under red pulp (RP) and white pulp (WP) was compared between WT and cKO spleen tissues (n=4, N=24). (J-M) Mononuclear cells harvested from WT and cKO spleen tissues were used for flow cytometry analysis. The proportion of CD11b/Gr-1⁺ myeloid cells (K), CD4/CD8⁺ T-cells (L) and B220⁺ B-cells (M) was compared between WT and cKO mice derived spleen tissues (n=6). Unpaired two-tailed Student's t-test was performed. * p<0.05, ** p<0.01, *** p<0.001, ns indicates not significant.

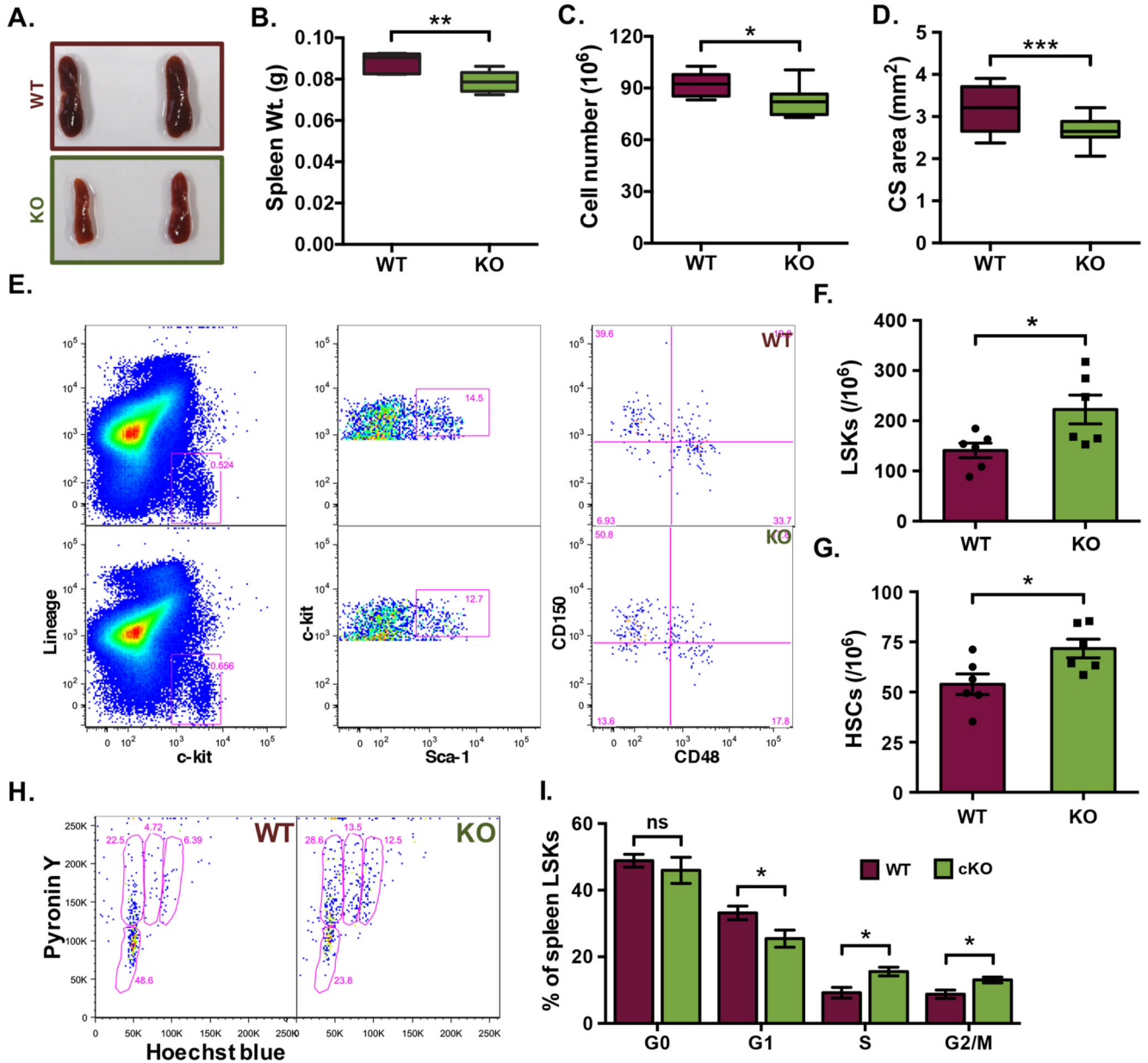


Figure 5. Loss of POSTN expression affects proliferation of hematopoietic progenitors in spleen (A) Spleen tissues from *Postn*^{+/+} (WT) and *Postn*^{-/-} (KO) mice were harvested. (B) Comparison of whole spleen weight from WT and KO mice. (C) The total number of MNCs from spleens of WT and KO mice. (D) Cross-sectional area quantified using transverse sections of spleen tissues from WT and KO mice. The formalin-fixed, paraffin-embedded tissues were used to cut 10µm sections that were used for H&E staining and analysis. (E-G) Quantification of frequency of various hematopoietic stem and progenitor cell populations in the spleen from WT and KO mice; (F) LSK cells, (G) primitive HSCs. (H) Cell cycle analysis of the spleen LSK cells. Total MNCs from spleen tissues were used to first label the cells with lineage, Sca-1 and c-kit antibodies followed by Hoechst 33342/Pyronin Y staining. Samples acquired on a flow cytometer were analyzed and LSK cells were gated

for further analysis for Hoechst 33342 and Pyronin Y intensity. (I) Comparison of the proportion of spleen LSK cells in various stages of cell cycle (n=6). Unpaired two-tailed Student's t-test was performed. * $p < 0.05$, ** $p < 0.01$, *** $p < 0.001$. ns indicates not significant.

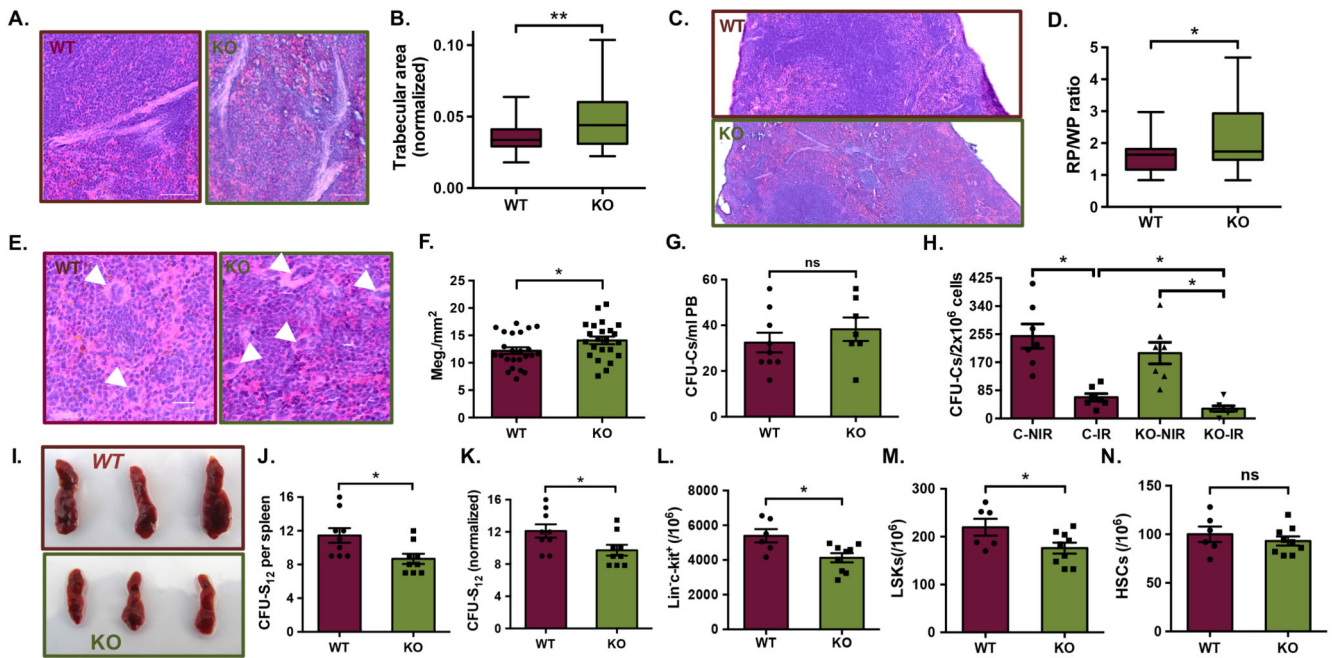


Figure 6. *Postn* deletion leads decline in spleen lympho-hematopoietic function

(A-D) Histological examination of spleen tissue sections from *Postn*^{+/+} (WT) and *Postn*^{-/-} (KO) mice. Tissues fixed in 4% paraformaldehyde were cut into 10 μ m sections and H&E staining was performed. Brightfield images were captured for histological analysis. (A) Examination of the trabecular area by H&E staining. (B) Quantification of trabecular area as proportion of the total cross-sectional area of spleen tissues from WT and KO mice. (C) H&E stained sections analyzed for spleen cross-sectional area under red and white pulp. (D) Comparison of the ratio of red versus white pulp in the spleen tissues from WT and KO mice. n=4, N=23-24

(E) Histological examination of the WT and KO spleen sections to identify megakaryocytes (white arrowheads) on the basis of morphological features. (F) Comparison of megakaryocyte frequency in spleen sections per mm² of the total cross-sectional area. n=4, N=24, unpaired two-tailed Student's t-test was performed, * p<0.05, ** p 0.01, ns indicates not significant.

(G) Methylcellulose-based colony assay performed to quantify HSPCs in peripheral blood of WT and KO mice. n=7, unpaired two-tailed Student's t-test, ns indicates not significant (p>0.05).

(H) *Postn*^{+/+} (C) and *Postn*^{-/-} (KO) mice with (IR) or without (NIR) radiation injury compared for HSPC frequency, using methylcellulose-based colony assay. Colony assays were performed one week after radiation injury and colonies were counted after 12 days. n=2, N=7 unpaired two-tailed Student's t-test, * p<0.05

(I) CFU-S₁₂ assay performed to assess the support potential of splenic niche for the incoming hematopoietic progenitors. Overall morphology of the WT and KO spleen tissues, 12 days after the mice received WT BM cells following lethal dose of irradiation.

(J) Comparison of the total number of spleen colonies in recipient WT and KO mice from CFU-S₁₂ assay.

(K) Comparison of the number of spleen colonies in WT and KO mice following normalization with the spleen weight.

(L-N) Flow cytometry analysis of spleen MNCs for comparison of the HSC sub-populations in spleen, following CFU-S₁₂ assay. Quantification of the frequency of various hematopoietic stem and progenitor cell populations in the spleen from WT and KO mice; (L) $\text{lin}^{-}\text{c-kit}^{+}$ cells, (M) LSK cells, (N) primitive HSCs.

Unpaired two-tailed Student's t-test was performed. $n=3$, $N=9$, t test: * $p<0.05$, ns indicates not significant.